



A novel organosilicon-based ionic plastic crystal as solid-state electrolyte for lithium-ion batteries*

Xin-yue ZHAO¹, Jing-lun WANG¹, Hao LUO¹, Hu-rong YAO², Chu-ying OUYANG², Ling-zhi ZHANG^{†‡1}

(¹Key Laboratory of Renewable Energy, Guangzhou Institute of Energy Conversion, Chinese Academy of Sciences, Guangzhou 510640, China)

(²College of Physics and Communication Electronics, Jiangxi Normal University, Nanchang 330022, China)

[†]E-mail: lzzhang@ms.giec.ac.cn

Received May 5, 2015; Revision accepted Aug. 5, 2015; Crosschecked Jan. 25, 2016

Abstract: A novel organosilicon-based ionic plastic crystal, *N,N,N*,-diethylmethyl-*N*-[(trimethylsilyl)methyl]ammonium bis-trifluoromethane sulfonimide ([DTMA][TFSI]) was designed and synthesized as solid-state electrolyte for lithium-ion batteries. The chemical structure and the physical and electrochemical properties were characterized in detail. The ionic conductivity of [DTMA][TFSI] was improved significantly by doping with lithium oxalyl difluoroborate (LiODFB) and propylene carbonate (PC). An optimized plastic crystal composite ([DTMA][TFSI]:LiODFB:PC=8:1:1 in molar ratio) as a solid-state electrolyte exhibited a decent cycling stability in LiFePO₄/Li half-cell, with a specific discharge capacity of 144 mA·h/g and capacity retention of 94% after 50 cycles at C/20.

Key words: Organosilicon, Ionic plastic crystal, Solid-state electrolyte, Lithium-ion battery
<http://dx.doi.org/10.1631/jzus.A1500099>

CLC number: O646

1 Introduction

Lithium-ion batteries have been widely used as power sources in portable electronic appliances because of their high energy density and long cycling life. However, commercial carbonate-based electrolytes, which are volatile and flammable, carry inherent drawbacks of leakage and safety problems for lithium-ion batteries (Zhang *et al.*, 2007; Kim *et al.*, 2008). Recently, solid-state electrolytes have received considerable interest due to their applications

covering a range of electrochemical devices, owing to their advantages of high safety, reduced leakage, excellent stability, as well as improved energy density and shape variability (Tarascon and Armand, 2001; Hammami *et al.*, 2003; Rana *et al.*, 2012). Among the solid-state electrolytes, organic ionic plastic crystals (OIPCs) represent a unique and complex family, members of which utilize a relatively large and symmetric organic cation in combination with an inorganic or organic anion. Used as a potential electrolyte for electrochemical devices, OIPCs possess many advantages such as excellent thermal stability, wide electrochemical window, high ionic conductivity, and nonflammability (MacFarlane and Forsyth, 2001; Wang *et al.*, 2013; Taniki *et al.*, 2014).

Recently, research on OIPCs mainly has focused on quaternary ammonium cations such as imidazolium, pyrrolidinium (Alarco *et al.*, 2004; Howlett *et al.*, 2011; Horike *et al.*, 2012), and quaternary phosphonium (Armel *et al.*, 2011). There are many studies on the structure and properties of new cations

[‡] Corresponding author

* Project supported by the Special Support Program of Guangdong Province for High-level Talents (No. 2014TX01N014), the Guangdong Provincial Project for Science & Technology (Nos. 2013B091300017 and 2014A050503050), the Guangzhou Municipal Project for Science & Technology (No. 201423/2014Y2-00219), and the Dongguan Municipal Collaboration Project for Industry & Science (No. 2013509104210), China

ORCID: Xin-yue ZHAO, <http://orcid.org/0000-0001-9097-771X>
 © Zhejiang University and Springer-Verlag Berlin Heidelberg 2016

and anions. The ionic liquids based on *N,N*-dialkyl-3-azabicyclo[3.2.2]nonanium cations exhibit plastic crystal properties and excellent lithium deposition-stripping behavior (Ruther *et al.*, 2007). Moriya *et al.* (2014) reported that new OIPCs, which were produced from cyclic perfluorosulfonylamide anion and cyano-substituted quaternary ammonium cations, had a wide plastic crystal temperature range, from about $-30\text{ }^{\circ}\text{C}$ to $250\text{ }^{\circ}\text{C}$. Armel *et al.* (2011) synthesized a range of OIPCs using phosphonium cations for the first time. To use OIPCs as potential solid-state electrolyte materials in lithium-ion batteries, the ionic conductivity and electrode compatibility of these materials have to be improved. Usually, these two properties could be circumvented by doping with a second component (such as lithium salts and nanoparticles) and using preconditioning process (Pringle, 2013; Unemoto *et al.*, 2014). Shekibi *et al.* (2012) have reported that *N*-ethyl-*N*-methylpyrrolidinium tetrafluoroborate ($[\text{C}_2\text{mpyr}][\text{BF}_4]$) was used as an ionic plastic crystal solid-state electrolyte for the lithium battery. Their results revealed that $[\text{C}_2\text{mpyr}][\text{BF}_4]$ doping with 10% LiBF_4 exhibited viable ionic conductivity at the level of 10^{-3} S/cm at $100\text{ }^{\circ}\text{C}$, and the discharge capacity in $\text{LiFePO}_4/\text{Li}$ cell was about $100\text{ mA}\cdot\text{h/g}$ at $80\text{ }^{\circ}\text{C}$ with current density of $C/10$. Sunarso *et al.* (2012) studied the preconditioning behavior by low current (0.01 mA/cm^2 at $50\text{ }^{\circ}\text{C}$) galvanostatic cycling of symmetrical lithium cells to improve the interfacial contact between the OIPCs and the electrodes. The $\text{LiFePO}_4/10\%\text{ LiNTf}_2$ in $[\text{C}_2\text{mpyr}][\text{NTf}_2]/\text{Li}$ cell showed a capacity of $129\text{ mA}\cdot\text{h/g}$ and retained $110\text{ mA}\cdot\text{h/g}$ after 50 cycles at $C/5$.

Organosilicon-based materials have attracted great attention as electrolytes for electrochemical energy storage devices due to their excellent thermal stability, viable ionic conductivity at low temperatures, low flammability, high electrochemical stability, and environmentally benign characters (Shirota and Castner, 2005; Zhang *et al.*, 2008; Rossi and West, 2009; Weng *et al.*, 2011). We have been dedicated to the design and synthesis of organosilicon-based electrolytes, including liquid electrolytes and ionic liquids, for applications in electrochemical energy storage devices such as lithium-ion batteries and supercapacitors (Zhong *et al.*, 2012; Qin *et al.*, 2013; Yan and Zhang, 2013; Yong *et al.*, 2014).

In this work, we report the synthesis of a novel

organosilicon-based ionic plastic crystal, *N,N,N*-diethylmethyl-*N*-[(trimethylsilyl)methyl] ammonium bistrifluoromethanesulfonylimide ($[\text{DTMA}][\text{TFSI}]$). The doping content of LiODFB and PC in $[\text{DTMA}][\text{TFSI}]$ was optimized. The electrochemical performances of the optimized composition as solid electrolyte were investigated in $\text{LiFePO}_4/\text{Li}$ half-cells by galvanostatic charge/discharge and electrochemical impedance spectroscopy (EIS) analysis.

2 Experimental

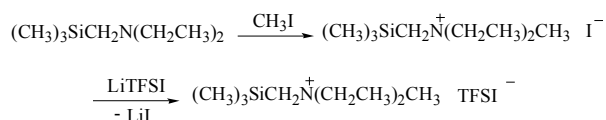
2.1 Materials

Methyl iodide (CH_3I , 99.5%) and silver nitrate (AgNO_3 , 99%) were purchased from Aladdin Co. (China). Lithium bis(trifluoromethanesulfonyl)imide (LiTFSI , lithium battery grade) was obtained from Sinoworo (China). LiODFB was purchased from Hongyang Chemical Ltd. (China). Propylene carbonate (PC) was commercially available from Zhangjiagang Guotai-Huarong Co. (China). LiFePO_4 was provided by Advanced Electronics Energy Ltd. (China).

2.2 Procedures for the synthesis of $[\text{DTMA}][\text{TFSI}]$

All reagents were used without further purification; solvents were dried using standard procedures. The organosilicon-based OIPC material used in this work was easily synthesized through a two-step route as outlined in Scheme 1. Typical procedures were as follows: *N*-[(trimethylsilyl)methyl]-*N,N*-diethylamine (0.10 mol, Hasegawa *et al.* (1988)) was dissolved in 200 ml tetrahydrofuran (THF) and cooled to $0\text{ }^{\circ}\text{C}$ in an ice bath; then, CH_3I (0.11 mol) was added dropwise. After stirring the mixture for 14 h at $60\text{ }^{\circ}\text{C}$, *N,N,N*-diethylmethyl-*N*-[(trimethylsilyl)methyl]ammonium iodide was obtained as a yellow powder through evaporation of the solvent. The iodide salt was purified by recrystallization with $\text{CH}_2\text{Cl}_2/\text{Et}_2\text{O}$ two times. In the second step, the iodide salt (0.090 mol) and LiTFSI (0.095 mol) were dissolved in 80 ml CH_2Cl_2 and 50 ml water. After the mixture was stirred for 1 d at room temperature, the CH_2Cl_2 phase was collected and washed with deionized water many times until no white precipitation was observed upon adding 1% AgNO_3 into the water phase. Then the CH_2Cl_2 was evaporated and

the target product was recrystallized two times with $\text{CH}_2\text{Cl}_2/\text{Et}_2\text{O}$, giving white needle-like crystals. The [DTMA][TFSI] was dried under vacuum at $100\text{ }^\circ\text{C}$, with overall yield of 88%.



Scheme 1 Route for synthesis of [DTMA][TFSI]

The chemical structure of [DTMA][TFSI] was confirmed by nuclear magnetic resonance (NMR) and Fourier transform infrared spectroscopy (FTIR):

^1H NMR of [DTMA][I] (600 MHz, CDCl_3 , δ): 3.54–3.58 (m, 4H, CCH_2N), 3.26 (s, 3H, NCH_3), 3.22 (s, 2H, SiCH_2N), 1.39–1.41 (t, 6H, CH_3CN^-), 0.30 (s, 9H, SiCH_3). ^1H NMR of [DTMA][TFSI] (600 MHz, CDCl_3 , δ): 3.32–3.36 (m, 4H, CCH_2N), 3.01 (s, 3H, NCH_3), 2.91 (s, 2H, SiCH_2N), 1.36–1.37 (t, 6H, CH_3CN), 0.28 (s, 9H, SiCH_3). ^{13}C NMR of [DTMA][TFSI] (150 MHz, CDCl_3 , δ): 0.42, 9.67, 52.14, 56.19, 60.80, 119.85 (q, $J_{\text{CF}}=214.8$). ^{29}Si NMR of [DTMA][TFSI] (120 MHz, CDCl_3 , δ): 21.78.

FTIR: 1056 cm^{-1} (S–N–S), 1194 cm^{-1} (C–F₃), $857/787\text{ cm}^{-1}$ (Si–CH₃).

2.3 Preparation of the composite plastic crystal materials and measurements

LiODFB salt was dried under vacuum for 24 h at $120\text{ }^\circ\text{C}$ before the organosilicon-based OIPC electrolyte preparation. The mixed electrolyte samples based on [DTMA][TFSI], LiODFB, and PC were prepared in the proportions shown in Table 1, and the mixture was stirred at $80\text{ }^\circ\text{C}$ for 2 h under argon atmosphere until a clear transparent viscous solution was obtained. These composite samples were allowed to cool to solid state under vacuum at $25\text{ }^\circ\text{C}$ and then transferred to a glove box for the next tests.

Table 1 Formulation of the composite samples

Sample	$x(\text{LiODFB})$ (%)	$x([\text{DTMA}][\text{TFSI}])$ (%)	$x(\text{PC})$ (%)
IPC1	0	100	0
IPC2	10	90	0
IPC3	20	80	0
IPC4	30	70	0
IPC5	10	80	10

Differential scanning calorimetry (DSC) was performed with a TA-Q100 instrument. All samples were loaded into hermetically sealed aluminum pans and scanned from $-100\text{ }^\circ\text{C}$ to $100\text{ }^\circ\text{C}$ at a scanning rate of $10\text{ }^\circ\text{C}/\text{min}$.

Conductivity measurements were performed using impedance spectroscopy technique. The sample was sandwiched between two stainless steel electrodes with 1.4 cm diameter and was assembled in an Ar-filled glove box. The impedance spectra were collected in the frequency range of 10 mHz to 2 MHz, with signal amplitude of 10 mV. The resistance value at which the low-frequency end of the semicircle crosses the x -axis of the complex impedance plot was obtained. The temperature was varied between $-20\text{ }^\circ\text{C}$ and $80\text{ }^\circ\text{C}$, allowing 30 min for thermal equilibration at each temperature. EIS results were obtained with Zennium/IM6 electrochemical workstation (Zahner, Germany).

2.4 Cell tests

The coin cells (CR2025) were assembled to test the electrochemical performance using LiFePO_4 cathode and lithium foil anode with the IPC5 composite sample as electrolyte. The LiFePO_4 electrode was prepared by coating a mixture of LiFePO_4 , carbon black, and poly(vinylidene fluoride) (PVDF), with a weight ratio of 80:10:10, on aluminum foil using *N*-methyl-2-pyrrolidone (NMP) as a solvent. The active material loading was about $5\text{ mg}/\text{cm}^2$. Both separators and cathodes were dried under vacuum at $80\text{ }^\circ\text{C}$ overnight. The cell assembly process was carried out in an argon-filled glove box with oxygen and moisture levels $<1\times 10^{-6}$. In order to make the electrodes, a separator (Celgard 2400, $\phi=1.6\text{ cm}$, $25\text{ }\mu\text{m}$ thickness) and plastic crystal electrolyte (about 110 mg per separator) were well impregnated, and the plastic crystal electrolyte was heated until melting for fabrication. The cells were placed inside high and low gimbals and galvanostatic charging-discharging cycled using a multichannel battery test system (NEWARE BTS-610). The charge and discharge cutoff voltage was from 2.5 V to 4 V. The EIS results were obtained with Zennium/IM6 electrochemical workstation (Zahner, Germany) at the end of charging ($\text{LiFePO}_4/\text{Li}$) with 10 mV perturbation amplitude applied in the frequency range of 10 mHz–1 MHz.

3 Results and discussion

3.1 DSC and ionic conductivity

LiODFB, as a lithium salt, is featured by its higher solubility, higher thermal stability, capability of passivating current collector, and forming a stable solid–electrolyte interface (SEI) on the surface of the electrode (Zhang, 2006). The DSC curves of [DTMA][TFSI] with different contents of LiODFB are shown in Fig. 1. The pure [DTMA][TFSI] sample (IPC1) showed plastic crystalline behavior over a wide temperature range, from approximately $-26\text{ }^{\circ}\text{C}$ to $54\text{ }^{\circ}\text{C}$, which is an advantage for its application in electrochemical devices at room temperature. The melting point of [DTMA][TFSI] decreased with increase in the doping contents of LiODFB from $54\text{ }^{\circ}\text{C}$ to $43\text{ }^{\circ}\text{C}$. The melting peaks became broader after doping with LiODFB, probably due to the formation of crystal defect and the fluctuation of the local crystallite packing and volume change during OIPC–liquid transition (Moriya *et al.*, 2014). Nevertheless, these composites remain in the plastic crystal states with clear solid–solid phase transitions and appear as an icy solid, even when LiODFB doping level increased up to 30%. It is known that adding an appropriate proportion of plasticizer can enhance ion mobility, hence increasing the ion conductivity of the electrolyte (Osman *et al.*, 2001; Glasse *et al.*, 2002). Therefore, IPC5 doped with 10% PC (commonly used plasticizer in gel polymer electrolytes) was prepared to further improve the ion conductivity. The plastic crystal temperature range of the sample IPC5 is from $-26\text{ }^{\circ}\text{C}$ to $43\text{ }^{\circ}\text{C}$. As can be seen from the DSC curve (Fig. 1), IPC5 can also remain in the solid state at room temperature.

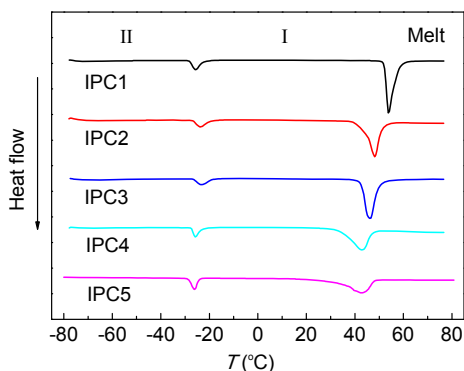


Fig. 1 DSC analysis of pure and [DTMA][TFSI] samples doped with LiODFB and PC

The phase transition temperature and the entropies of fusion (ΔS) of [DTMA][TFSI] doping with different contents of LiODFB are summarized in Table 2. According to Timmermans (1961)'s criterion, the entropy of fusion for plastic crystal is considered to be $<20\text{ J}/(\text{mol}\cdot\text{K})$. However, the entropy of melting can be higher for OIPCs because one of its ion species may exhibit rotational motions (MacFarlane *et al.*, 2001). The entropy of fusion of [DTMA][TFSI] turned out to be $63\text{ J}/(\text{mol}\cdot\text{K})$, doping with LiODFB resulted in decreasing the entropy of fusion. Similarly, $[\text{P}_{1444}][\text{BF}_4]$ and $[\text{P}_{1444}][\text{SCN}]$ salts exhibit quite low conductivities, consistent with their high entropies of fusion ($44\text{--}45\text{ J}/(\text{mol}\cdot\text{K})$), demonstrating a relatively ordered phase (Armel *et al.*, 2011). The decreased entropy of LiODFB/[DTMA][TFSI] suggests that LiODFB might affect the crystallinity of the plastic crystal, probably owing to the formation of solid solutions as observed in LiTFSI-pyrrolidinium family (Forsyth *et al.*, 2000). IPC5 exhibits a similar phase transition entropy as IPC3, having the same doping level of 20%. However, the melting entropy of IPC5 was slightly lower than that of IPC3, possibly because the PC liquid region could be housed within the extensive dislocation networks known to exist in the plastic crystal phase (Abu-Lebdeh *et al.*, 2004).

Table 2 Phase transition temperature and the entropies of the samples

Sample	Phase transition			
	II–I		I–Melt	
	$T\text{ (}^{\circ}\text{C)}$	$\Delta S\text{ (J}/(\text{mol}\cdot\text{K}))$	$T\text{ (}^{\circ}\text{C)}$	$\Delta S\text{ (J}/(\text{mol}\cdot\text{K}))$
IPC1	-26	15	54	63
IPC2	-24	13	48	60
IPC3	-23	11	46	58
IPC4	-26	9	43	43
IPC5	-26	12	43	53

Data of T and ΔS have a margin of error of ± 1 and $\pm 5\%$, respectively

The temperature dependence of the conductivities of [DTMA][TFSI] and the ternary composite [DTMA][TFSI]/LiODFB/PC is shown in Fig. 2. The conductivity of IPC1 was $3\times 10^{-8}\text{ S}/\text{cm}$ ($25\text{ }^{\circ}\text{C}$). However, after doping with 10% LiODFB, IPC2 showed a conductivity of $4\times 10^{-8}\text{ S}/\text{cm}$, not much improved compared with pure IPC1. But the conductivity of the sample IPC5 with 10% LiODFB and

10% PC in [DTMA][TFSI] was obviously improved. As expected, the sample IPC5 showed a significantly increased conductivity of 1×10^{-4} S/cm. The conductivities of both IPC1 and IPC5 were increased with the increase of the temperature, and the conductivities of the samples reached about the same level at 60 °C, where the two samples were in liquid states. The composite [DTMA][TFSI]/LiODFB/PC sample exhibited moderate conductivity and could be maintained in the solid state at room temperature (Fig. 3), so it was chosen as solid-state electrolyte for the following electrochemical tests.

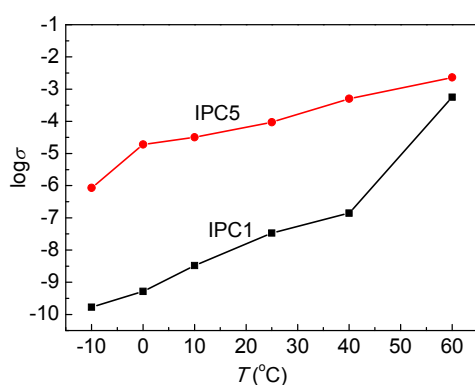


Fig. 2 Temperature dependence of conductivity of IPC1 and IPC5

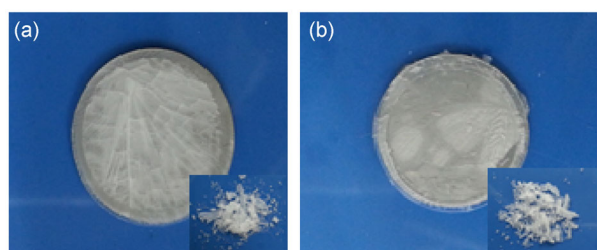


Fig. 3 Photographs of IPC1 (a) and IPC5 (b) at room temperature

3.2 Cell tests

The electrochemical performance of the sample IPC5 as solid-state electrolyte for LiFePO₄/Li half-cells was investigated in detail. Fig. 4 presents the initial and the third galvanostatic charge-discharge curves for the LiFePO₄/IPC5/Li cell cycled with the current density of C/20 (8 mA/g) and the cutoff voltage range of 2.5–4.0 V at room temperature. The cell showed an initial charge–discharge capacity of 156/137 mA·h/g and a Coulombic efficiency of 88%. At the third cycle, the cell delivered a discharge capacity of 144 mA·h/g with a higher Coulombic efficiency of 99%. Moreover, the polarization was also

decreased in the third cycle, which could be observed distinctly in Fig. 4. EIS was used to characterize the impedance properties of the LiFePO₄/IPC5/Li cell (Fig. 5). The Nyquist plots of the impedance spectra consisted of one large depressed semicircle in the high-frequency region and a straight line in the low-frequency region, which correspond to the charge transfer process and Warburg diffusion impedance, respectively. Comparing the impedance spectra of the cell after the first and the third cycles, it was observed that the charge transfer impedance decreased from 800 Ω to 360 Ω after three cycles. The decrease of impedance with increasing cycles might be attributed to the formation of a passivation layer and good contact compatibility between lithium and the solid-state electrolyte interface (Sunarso *et al.*, 2012), which could be the reason for the capacity increase during the first three cycles.

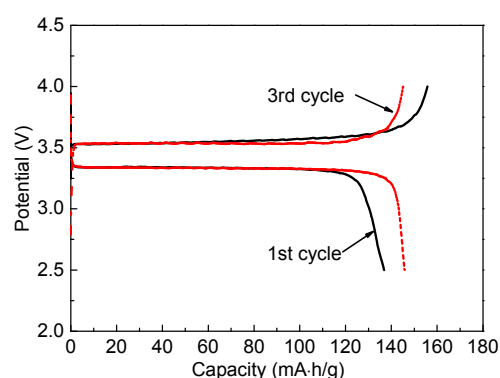


Fig. 4 Galvanostatic cycle curves of LiFePO₄/IPC5/Li cell for the first cycle and the third cycle

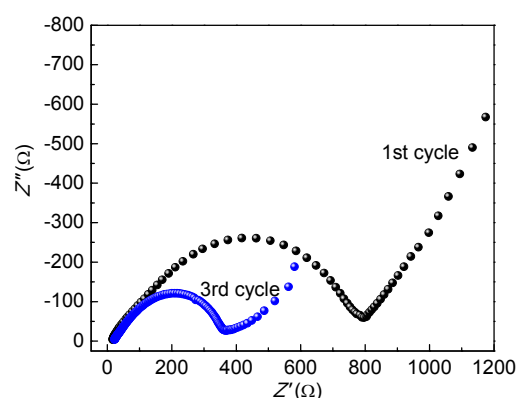


Fig. 5 Impedance spectra of the cell after the first and the third cycles

The cycling performance of the LiFePO₄/IPC5/Li cell at the current rate of C/20 is displayed in

Fig. 6. The cell exhibited excellent cycle performance with specific discharge capacity of 144 mA·h/g and Coulombic efficiency of 99% after 50 cycles, and the overall capacity retention turned out to be 94%. The rate performance of LiFePO₄/IPC5/Li cell at various current densities was measured at room temperature (Fig. 7). At C/10, C/12, C/20, and C/24, the cell displayed a specific capacity of 100 mA·h/g, 126 mA·h/g, 143 mA·h/g, and 158 mA·h/g, respectively. However, the specific capacity of the cell faded rapidly when the current density was above C/8 rate, which may be related to the limited ionic conductivity of the solid-state electrolyte and the charge transfer resistance of the SEI film.

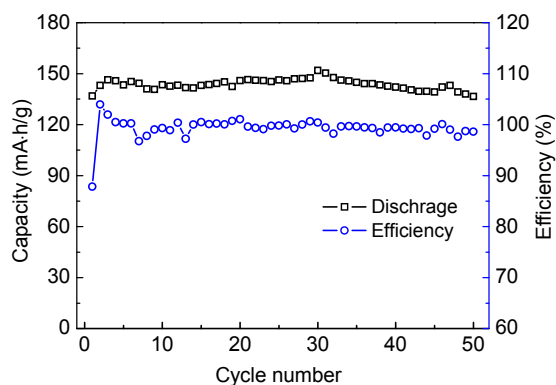


Fig. 6 Specific discharge capacity (a) and efficiency (b) vs. cycle number for LiFePO₄/IPC5/Li cell at room temperature at C/20

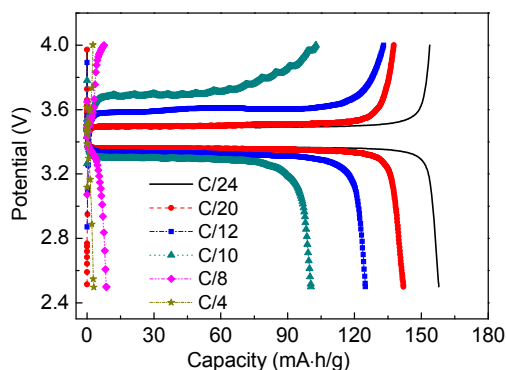


Fig. 7 Charge-discharge capacity at different discharge rates for the LiFePO₄/IPC5/Li cell at room temperature

4 Conclusions

A novel organosilicon-based ionic plastic crystal electrolyte [DTMA][TFSI] was synthesized and its plastic crystal temperature range was from $-26\text{ }^{\circ}\text{C}$

to $54\text{ }^{\circ}\text{C}$. By doping the neat OIPC material with 10% LiODFB and 10% PC, the [DTMA][TFSI] composite showed a significantly increased ionic conductivity of $1 \times 10^{-4}\text{ S/cm}$ at $25\text{ }^{\circ}\text{C}$, which is sufficient to expect operation of battery cells to be possible at room temperature. The LiFePO₄/Li cell with this plastic crystal as solid-state electrolyte exhibited good cycle performance, with specific capacity of 144 mA·h/g and Coulombic efficiency of 99% at current density of C/20, and retained 94% capacity after 50 cycles. These data demonstrate that these new organosilicon-based ionic plastic crystal composites have considerable potential as solid-state electrolyte materials for use in lithium-ion batteries, particularly in Li metal batteries demanding a stable surface of Li metal as an electrochemical device with equally high energy density as Li-sulfur and Li-air batteries.

References

- Abu-Lebdeh, Y., Abouimrane, A., Alarco, P.J., et al., 2004. Ambient temperature proton conducting plastic crystal electrolytes. *Electrochemistry Communications*, **6**(4): 432-434.
<http://dx.doi.org/10.1016/j.elecom.2004.02.015>
- Alarco, P.J., Abu-Lebdeh, Y., Ravet, N., et al., 2004. Lithium conducting pyrazolium imides plastic crystals: a new solid state electrolyte matrix. *Solid State Ionics*, **172**(1-4): 53-56.
<http://dx.doi.org/10.1016/j.ssi.2004.02.029>
- Armel, V., Velayutham, D., Sun, J.Z., et al., 2011. Ionic liquids and organic ionic plastic crystals utilizing small phosphonium cations. *Journal of Materials Chemistry*, **21**(21):7640-7650.
<http://dx.doi.org/10.1039/c1jm10417a>
- Forsyth, M., Huang, J., MacFarlane, D.R., 2000. Lithium doped *N*-methyl-*N*-ethylpyrrolidinium bis(trifluoromethanesulfonyl)amide fast-ion conducting plastic crystals. *Journal of Materials Chemistry*, **10**(10):2259-2265.
<http://dx.doi.org/10.1039/b003168m>
- Glasse, M.D., Idris, R., Latham, R.J., et al., 2002. Polymer electrolytes based on modified natural rubber. *Solid State Ionics*, **147**(3-4):289-294.
[http://dx.doi.org/10.1016/S0167-2738\(02\)00024-3](http://dx.doi.org/10.1016/S0167-2738(02)00024-3)
- Hammami, A., Raymond, N., Armand, M., 2003. Runaway risk of forming toxic compounds. *Nature*, **424**(6949): 635-636.
<http://dx.doi.org/10.1038/424635b>
- Hasegawa, E., Brumfield, M.A., Mariano, P.S., et al., 1988. Photoadditions of ethers, thioethers, and amines to 9, 10-dicyanoanthracene by electron-transfer pathways. *Journal of Organic Chemistry*, **53**(23):5435-5442.
<http://dx.doi.org/10.1021/jo00258a007>

- Horike, S., Umeyama, D., Inukai, M., et al., 2012. Coordination-network-based ionic plastic crystal for anhydrous proton conductivity. *Journal of the American Chemical Society*, **134**(18):7612-7615.
<http://dx.doi.org/10.1021/ja301875x>
- Howlett, P.C., Sunarso, J., Shekibi, Y., et al., 2011. On the use of organic ionic plastic crystals in all solid-state lithium metal batteries. *Solid State Ionics*, **204-205**:73-79.
<http://dx.doi.org/10.1016/j.ssi.2011.09.012>
- Kim, H., Nguyen, D.Q., Bae, H.W., et al., 2008. Effect of ether group on the electrochemical stability of zwitterionic imidazolium compounds. *Electrochemistry Communications*, **10**(11):1761-1764.
<http://dx.doi.org/10.1016/j.elecom.2008.09.006>
- MacFarlane, D.R., Forsyth, M., 2001. Plastic crystal electrolyte materials: new perspectives on solid state ionics. *Advanced Materials*, **13**(12-13):957-966.
[http://dx.doi.org/10.1002/15214095\(200107\)13:12/13<957::AID-ADMA957>3.0.CO;2-#](http://dx.doi.org/10.1002/15214095(200107)13:12/13<957::AID-ADMA957>3.0.CO;2-#)
- MacFarlane, D.R., Meakin, P., Amini, N., et al., 2001. Structural studies of ambient temperature plastic crystal ion conductors. *Journal of Physics: Condensed Matter*, **13**(36):8257-8267.
<http://dx.doi.org/10.1088/0953-8984/13/36/303>
- Moriya, M., Watanabe, T., Nabeno, S., et al., 2014. Crystal structure and solid-state ionic conductivity of cyclic sulfonamide salts with cyano-substituted quaternary ammonium cations. *Chemistry Letters*, **43**(1):108-110.
<http://dx.doi.org/10.1246/cl.130874>
- Osman, Z., Ibrahim, Z.A., Arof, A.K., 2001. Conductivity enhancement due to ion dissociation in plasticized chitosan based polymer electrolytes. *Carbohydrate Polymers*, **44**(2):167-173.
[http://dx.doi.org/10.1016/S0144-8617\(00\)00236-8](http://dx.doi.org/10.1016/S0144-8617(00)00236-8)
- Pringle, J.M., 2013. Recent progress in the development and use of organic ionic plastic crystal electrolytes. *Physical Chemistry Chemical Physics*, **15**(5):1339-1351.
<http://dx.doi.org/10.1039/C2CP43267F>
- Qin, X.Y., Wang, J.L., Tang, D.P., et al., 2013. Triethoxysilane with oligo(ethylene oxide) substituent as film forming additive for graphite anode. *Journal of Zhejiang University-SCIENCE A (Applied Physics & Engineering)*, **14**(7):514-519.
<http://dx.doi.org/10.1631/jzus.A1300026>
- Rana, U.A., Forsyth, M., MacFarlane, D.R., et al., 2012. Toward protic ionic liquid and organic ionic plastic crystal electrolytes for fuel cells. *Electrochimica Acta*, **84**:213-222.
<http://dx.doi.org/10.1016/j.electacta.2012.03.058>
- Rossi, N.A.A., West, R., 2009. Silicon-containing liquid polymer electrolytes for application in lithium ion batteries. *Polymer International*, **58**(3):267-272.
<http://dx.doi.org/10.1002/pi.2523>
- Ruther, T., Huang, J., Hollenkamp, A.F., 2007. A new family of ionic liquids based on *N,N*-dialkyl-3-azabicyclo[3.2.2]nonanium cations: organic plastic crystal behaviour and highly reversible lithium metal electrodeposition. *Chemical Communications*, **48**:5226-5228.
<http://dx.doi.org/10.1039/b709772g>
- Shekibi, Y., Ruther, T., Huang, J.H., et al., 2012. Realisation of an all solid state lithium battery using solid high temperature plastic crystal electrolytes exhibiting liquid like conductivity. *Physical Chemistry Chemical Physics*, **14**(13):4597-4604.
<http://dx.doi.org/10.1039/c2cp24077g>
- Shirota, H., Castner, E.W., 2005. Why are viscosities lower for ionic liquids with $-\text{CH}_2\text{Si}(\text{CH}_3)_3$ vs $-\text{CH}_2\text{C}(\text{CH}_3)_3$ substitutions on the imidazolium cations? *Journal of Physical Chemistry B*, **109**(46):21576-21585.
<http://dx.doi.org/10.1021/jp053930j>
- Sunarso, J., Shekibi, Y., Efthimiadis, J., et al., 2012. Optimising organic ionic plastic crystal electrolyte for all solid-state and higher than ambient temperature lithium batteries. *Journal of Solid State Electrochemistry*, **16**(5):1841-1848.
<http://dx.doi.org/10.1007/s10008-011-1566-6>
- Taniki, R., Matsumoto, K., Nohira, T., et al., 2014. All solid-state electrochemical capacitors using *N,N*-dimethylpyrrolidinium fluorohydrogenate as ionic plastic crystal electrolyte. *Journal of Power Sources*, **245**:758-763.
<http://dx.doi.org/10.1016/j.jpowsour.2013.07.020>
- Tarascon, J.M., Armand, M., 2001. Issues and challenges facing rechargeable lithium batteries. *Nature*, **414**(6861):359-367.
<http://dx.doi.org/10.1038/35104644>
- Timmermans, J., 1961. Plastic crystals—a historical review. *Journal of Physics and Chemistry of Solids*, **18**(1):1-8.
[http://dx.doi.org/10.1016/0022-3697\(61\)90076-2](http://dx.doi.org/10.1016/0022-3697(61)90076-2)
- Unemoto, A., Gambe, Y., Komatsu, D., et al., 2014. Development of high capacity all-solid-state lithium battery using quasi-solid-state electrolyte containing tetraglyme-Li-TFSA equimolar complexes. *Solid State Ionics*, **262**:765-768.
<http://dx.doi.org/10.1016/j.ssi.2013.09.043>
- Wang, Y.F., Zhang, J.M., Cui, X.R., et al., 2013. A novel organic ionic plastic crystal electrolyte for solid-state dye-sensitized solar cells. *Electrochimica Acta*, **112**:247-251.
<http://dx.doi.org/10.1016/j.electacta.2013.08.159>
- Weng, W., Zhang, Z.C., Lu, J., et al., 2011. A disiloxane-functionalized phosphonium-based ionic liquid as electrolyte for lithium-ion batteries. *Chemical Communications*, **47**(43):11969-11971.
<http://dx.doi.org/10.1039/c1cc15331e>
- Yan, X.D., Zhang, L.Z., 2013. Polyethylene glycol-modified poly(3,4-ethylene dioxythiophene):poly(styrene sulfonate) counter electrodes for dye-sensitized solar cell. *Journal of Applied Electrochemistry*, **43**(6):605-610.
<http://dx.doi.org/10.1007/s10800-013-0544-3>
- Yong, T.Q., Wang, J.L., Mai, Y.J., et al., 2014. Organosilicon compounds containing nitrile and oligo(ethylene oxide) substituents as safe electrolytes for high-voltage lithium-ion batteries. *Journal of Power Sources*, **254**:29-32.
<http://dx.doi.org/10.1016/j.jpowsour.2013.12.087>
- Zhang, H.P., Fu, L.J., Wu, Y.P., et al., 2007. Changes of

LiCoO₂ cathode material for lithium-ion battery during long cycling. *Electrochemical and Solid-State Letters*, **10**(12):A283-A285.

<http://dx.doi.org/10.1149/1.2789404>

Zhang, L.Z., Zhang, Z.C., Haring, S., et al., 2008. Highly conductive trimethylsilyl oligo(ethylene oxide) electrolytes for energy storage applications. *Journal of Materials Chemistry*, **18**(31):3713-3717.

<http://dx.doi.org/10.1039/b806290k>

Zhang, S.S., 2006. An unique lithium salt for the improved electrolyte of Li-ion battery. *Electrochemistry Communications*, **8**(9):1423-1428.

<http://dx.doi.org/10.1016/j.elecom.2006.06.016>

Zhong, H.X., Zhao, C.B., Luo, H., et al., 2012. Novel organo-silicon ionic liquid based electrolytes for supercapacitors. *Acta Physico-Chimica Sinica*, **28**(11):2641-2647.

<http://dx.doi.org/10.3866/PKU.WHXB201207181>

中文概要

题目: 新型有机硅基离子塑晶材料作为固态电解质用于锂离子电池

目的: 合成新型的有机硅基离子塑晶材料 [DTMA][TFSI], 测试材料的物理和电化学性能, 研究其掺杂改性并作为固态电解质用于锂离子电池。

创新点: 1. 合成新型的有机硅基离子型塑晶材料; 2. 将三元复合塑晶材料作为固态电解质在室温下用于锂离子电池。

方法: 1. 通过热性能分析, 得到材料的塑晶温度区间和融化焓值 (图 1 和表 1); 2. 通过电导率测试, 确定塑晶掺杂对导电性能的影响 (图 2); 3. 通过对扣式电池的充放电性能、倍率性能、循环性能以及阻抗的测试 (图 4~7), 得到塑晶复合物作为固态电解质的电化学性能以及电池循环的稳定性和可逆性。

结论: 1. 合成新型有机硅基离子塑晶材料 [DTMA][TFSI], 塑晶温度区间为 -26 °C 到 54 °C; 2. 在纯塑晶 IPC 中添加 10% LiODFB 和 10% PC, 得到复合物的电导率为 1×10^{-4} S/cm, 提高塑晶作为固态电解质在室温下应用的可行性; 3. 将复合物用于 LiFePO₄/Li 半电池测试, 在 C/20 倍率下, 电池的放电比容量为 144 mA·h/g, 库伦效率为 99%。在 50 次循环后, 容量保持率为 94%; 4. 测试结果表明, 新型有机硅基离子塑晶的复合物可作为固态电解质材料应用于锂离子电池, 以及更高能量密度的锂-硫和锂-空电池。

关键词: 有机硅; 离子塑晶; 固态电解质; 锂离子电池